Mechanism of Inhibition of Skeletal Muscle Actomyosin by *N*-Benzyl-*p*-toluenesulfonamide†

M. Alexander Shaw, E. Michael Ostap, and Yale E. Goldman*

Pennsylvania Muscle Institute, University of Pennsylvania, Philadelphia, Pennsylvania 19104

Received October 8, 2002; Revised Manuscript Received March 22, 2003

ABSTRACT: *N*-Benzyl-*p*-toluenesulfonamide (BTS) is a small organic molecule that specifically inhibits the contraction of fast skeletal muscle fibers. To determine the mechanism of inhibition by BTS, we performed a kinetic analysis of its effects on the elementary steps of the actomyosin subfragment-1 ATPase cycle. BTS decreases the steady-state acto-S1 ATPase rate approximately 10-fold and increases the actin concentration for half-maximal activation. BTS primarily affects three of the elementary steps of the reaction pathway. It decreases the rate of P_i release >20-fold in the absence of actin and >100-fold in the presence of actin. It decreases the rate of S1·ADP dissociation from 3.9 to 0.8 s^{-1} while decreasing the S1·ADP dissociation constant from 2.3 to 0.8 μM. BTS weakens the apparent affinity of S1·ADP for actin, increasing the K_d from 7.0 to 29.5 μM. ATP binding to S1, hydrolysis, and the affinity of nucleotide-free S1 for actin are unaffected by BTS. Kinetic modeling indicates that the binding of BTS to myosin depends on actin association/dissociation and on nucleotide state. Our results suggest that the reduction of the acto-S1 ATPase rate is due to the inhibition of P_i release, and the suppression of tension is due to inhibition of P_i release in conjunction with the decreased apparent affinity of S1·ADP·P_i and S1·ADP for actin.

N-Benzyl-*p*-toluenesulfonamide (BTS) is a small organic molecule that inhibits active tension generation in rabbit fast-twitch skeletal muscle fibers at micromolar concentrations (*1*). This inhibition is very specific for fast skeletal muscle: the inhibition of rat myocardium or rabbit slow-twitch muscle fibers is much weaker. Similarly, while BTS markedly inhibits the actin-activated ATPase of subfragment 1 (S1) of rabbit skeletal muscle myosin, it does not inhibit human platelet myosin II. Although the molecule 2,3-butanedione monoxime (BDM) has also been shown to inhibit skeletal muscle myosin-II (*2*), while not significantly inhibiting other members of the myosin family (*3*, *4*), it is a low-affinity reagent ($K_I \approx 4$ mM) that affects proteins other than myosin (*5*). Thus, BTS is a more potent and specific inhibitor of fast-twitch muscle myosin than BDM. BTS may be useful in studies of muscle fiber contraction or myosin II structure−function relationships.

Tension production by actively contracting rabbit psoas fast-twitch fibers is suppressed 97% by BTS with an IC_{50} of 3 μM. Additionally, acto-HMM cosedimentation assays indicated that BTS weakens the affinity of myosin for actin. BTS does not, however, greatly affect the shortening velocity of unloaded psoas fibers (*1*). Taken together, these results suggest that BTS disrupts the actomyosin interaction during muscle fiber contraction.

We performed kinetic studies of ATP hydrolysis by rabbit S1 in the presence of BTS to determine the mechanism of its inhibitory actions in more detail and to relate these effects to contraction in fibers. The kinetic mechanism of ATP hydrolysis by myosin has been well characterized in the absence of BTS (Scheme 1, refs *6*−*11*). We measured key kinetic parameters defined in Scheme 1 in the absence and in the presence of BTS. The overall steady-state actin-activated ATPase was measured with an NADH-coupled enzymatic assay. Using internal tryptophan fluorescence, we measured the rate of ATP binding to S1 (k_{+1d}), the rate of ATP cleavage steps ($k_{+2d} + k_{-2d}$), the single-turnover rate of ATP hydrolysis (k_{+3d}), and the dissociation constant of ADP binding to S1 (K_{4d}). The fluorescence change of pyrene-labeled actin upon strong binding of S1 was used to measure the dissociation constants of S1 and S1·ADP for actin (K_5 and K_8, respectively), as well as the dissociation constant of ADP binding to acto-S1 (K_{4a}). The likely mechanism of inhibition of fiber contraction is a suppression of P_i release (k_{3a}). Some of these results have already been presented in abstract form (*12*).

MATERIALS AND METHODS

Reagents. *N*-Benzyl-*p*-toluenesulfonamide (BTS) was generously provided by Dr. Tim Mitchison and Dr. Aaron Straight (Harvard Medical School, Boston, MA) or purchased from Sigma Rare Chemicals (St. Louis, MO). Ultrapure ATP (>99%), NADH, phospho(enol) pyruvate, pyruvate kinase, and lactic dehydrogenase were purchased from Sigma. ADP was purchased from Sigma and purified to >99% by anion-exchange chromatography. All other chemicals and reagents were reagent grade.

Proteins. Myosin was purified from rabbit leg and back muscle according to standard procedures (*13*). Myosin

† Supported by NIH grant P01 HL15835.

* Address correspondence to this author at Pennsylvania Muscle Institute, D700 Richards Building/3700 Hamilton Walk, Philadelphia, PA 19104-6083. Phone: (215) 898-4017. Fax: (215) 898-2653. E-mail: goldmany@mail.med.upenn.edu.

10.1021/bi026964f CCC: $25.00
Published on Web 05/01/2003

Scheme 1

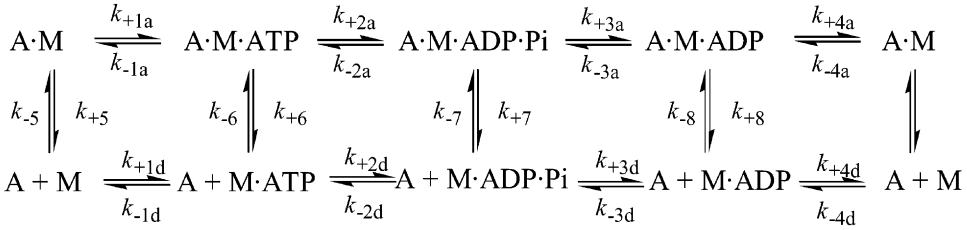

subfragment 1 (S1) was produced from rabbit skeletal muscle myosin by chymotryptic digestion (*14*, *15*). S1 was stored at −80 °C in the presence of 3 mg of sucrose/mg of S1. Prior to use, S1 was thawed slowly and dialyzed overnight into the experimental buffer. Actin was purified from acetone powder as previously described (*16*) and dialyzed overnight into the experimental buffer. Pyrene-labeled actin was produced according to the method described by Pollard (*17*). Phosphate-binding protein (P_iBP) was expressed, purified, and fluorescently labeled as previously described (*18*, *19*).

Steady-State ATPases. ATPase assays were performed using an NADH-coupled assay monitoring absorbance at 340 nm. These experiments were performed using either an Applied Photophysics stopped-flow apparatus or a standard UV/vis spectrophotometer at 25 °C. ATPase reactions contained 50 nM S1 in buffer A [10 mM imidazole (pH 7.0), 2 mM $MgCl_2$, 1 mM EGTA, and 1 mM DTT] containing 100 U/mL pyruvate kinase, 20 U/mL lactic dehydrogenase, 200 μM NADH, and 500 μM phospho(enol) pyruvate. Actin concentrations varied from 0 to 150 μM. Reactions were initiated by the addition of 2 mM MgATP.

Internal Tryptophan Fluorescence. Experiments were performed using an Applied Photophysics stopped-flow apparatus. Protein fluorescence was excited at 295 nm and collected through a 320-nm long-pass emission filter. Experiments were performed in either buffer A (see above) or buffer B [20 mM Tris-HCl (pH 7.0), 200 mM KCl, 2 mM $MgCl_2$, and 1 mM DTT] at 25 °C.

Pyrene-Actin Fluorescence. The extent of strong S1 binding to actin under various conditions was measured by fluorescence quenching of pyrene-labeled actin in buffer B at 25 °C. Steady-state measurements were performed on a standard fluorometer using an excitation wavelength of 365 nm. Emission was measured through a 400-nm cutoff filter and a monochromator set to 412 nm. Transient experiments were performed on an Applied Photophysics stopped-flow apparatus, exciting at 365 nm and monitoring emission through a 400-nm cutoff filter.

Phosphate Release. Transient phosphate (P_i) release was measured using a fluorescently labeled mutant of phosphate-binding protein (P_iBP; *18*, *19*) with the stopped flow in sequential mixing mode and using a 440-nm long-pass filter (λ_{ex} = 425 nm). The dead time of the instrument in this configuration was ~2 ms. Contaminating phosphate was removed from syringes, plastic ware, and the stopped-flow apparatus by incubating overnight with 0.5 mM 7-methylguanosine and 1 U/mL nucleoside phosphorylase in buffer A. Background phosphate was removed from experimental solutions by incubating with 0.1 mM 7-methylguanosine and 0.02 U/mL nucleoside phosphorylase.

Analysis and Kinetic Modeling. Experimental transients were fitted with software supplied with the stopped-flow instrument or with SigmaPlot (SPSS Science). Kinetic modeling was performed using MathCad (Mathsoft, Inc.).

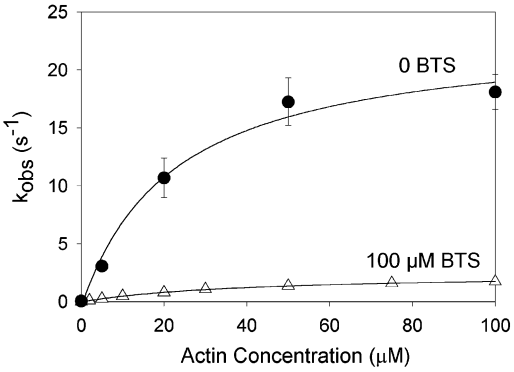

FIGURE 1: Actin-activated ATPase curves in the absence of BTS and in the presence of 100 μM BTS. Final reaction concentrations were 50 nM S1, 0−100 μM actin, 10 mM imidazole (pH 7.0), 4 mM $MgCl_2$, 1 mM DTT, 2 mM ATP, 20 U/mL lactate dehydrogenase, 100 U/mL pyruvate kinase, 200 μM NADH, 500 μM phospho(enol)pyruvate, and 0 or 100 μM BTS. Temperature was maintained at 25 °C. BTS (open symbols) inhibits the rate of ATP hydrolysis by rabbit S1 and increases the K_{ATPase} value.

RESULTS

Steady-State ATPases. BTS (100 μM) decreases the maximum rate of actin-activated myosin ATPase (V_{max}) approximately 10-fold, from 23.3 to 2.5 s^{-1} (Figure 1, Table 1). It also increases the actin concentration required to reach the half-maximum ATPase rate (K_{ATPase}) from 22.3 to 39.4 μM. These data indicate that BTS has two effects on steady-state ATPase activity. It slows the rate-limiting step of actin-activated ATP hydrolysis, and it weakens the apparent affinity of S1 for actin in the presence of ATP. The K_I of BTS for ATP hydrolysis is approximately 8 μM in the absence of actin and ~3 μM in the presence of 24 μM actin (not shown). These results agree with previous work (*1*). All remaining experiments were performed at either 25 or 100 μM BTS.

Rates of ATP Binding and Hydrolysis (k_{+1d}, $k_{+2d} + k_{-2d}$). We used enhancement of intrinsic tryptophan fluorescence of S1 to measure rates of ATP binding and hydrolysis (*20*). The rates of fluorescence increase as a function of ATP are similar in the presence and in the absence of BTS (Figure 2, open and closed symbols, respectively). The maximum rate of the fluorescence enhancement of S1 at high ATP concentration reports the rate of the ATP cleavage step ($k_{+2d} + k_{-2d}$) and is 157 ± 7 s^{-1} in the absence of BTS and 124 ± 5 s^{-1} in the presence of 25 μM BTS. The association rate constant for ATP binding (k_{+1d}) determined from the initial slope (Figure 2B) is 9.0 × 10^6 M^{-1} s^{-1} in the absence of BTS and 8.2 × 10^6 M^{-1} s^{-1} in the presence of 25 μM BTS.

Table 1: Kinetic Parameters of ATP Hydrolysis with and without BTS

	without BTS	with BTS[a]
V_{max}, s^{-1} [b]	23.3 ± 1.8	2.5 ± 0.3
K_{ATPase}, μM[b]	22.3 ± 3.2	39.4 ± 2.0
k_{+1a}, μM^{-1} [c]	(1.9 ± 0.02) × 10^6	(1.8 ± 0.09) × 10^6
k_{+1d}, μM^{-1} s^{-1} [c]	9.0	8.2
$k_{+2d} + k_{-2d}$, s^{-1} [c]	157 ± 7	124 ± 5
k_{+3a}^{app}, s^{-1} [b,d]	53 ± 1.0	0.37 ± 0.01
k_{+3d}, s^{-1} [b]	0.105 ± 0.004	<0.005
K_{4a}, M^{-1} [c]	(3.3 ± 0.3) × 10^3	(3.4 ± 0.3) × 10^3
K_{4d}, μM[c]	2.3	0.8
K_p, μM[c]	38 ± 5.0	10 ± 0.7
k_{+q}, s^{-1} [c]	63 ± 2.4	9.9 ± 0.2
k_{-q}, s^{-1} [c]	3.9 ± 0.03	0.8 ± 0.02
$K_p k_{+q}$, μM^{-1} s^{-1} [c]	1.7	1.0
K_5 (slow phase), μM[c]	0.17	0.19
K_5 (fast phase), μM[c]	0.036	0.042
K_{+5}, s^{-1} [c]	0.29 ± 0.006	0.31 ± 0.007
k_{-5} (slow phase), μM^{-1} s^{-1} [c]	1.7 ± 0.05	1.6 ± 0.14
k_{-5} (fast phase), μM^{-1} s^{-1} [c]	8.1 ± 0.34	7.3 ± 0.79
K_8, μM[c]	7.0 ± 0.8	29 ± 5.6[e]

[a] The BTS concentration was 100 μM, except for the determinations of k_{+1a}, k_{+1d}, and $k_{+2d} + k_{-2d}$, where it was 25 μM. [b] Buffer A: 10 mM imidazole (pH 7.0), 2 mM $MgCl_2$, 1 mM EGTA, and 1 mM DTT. [c] Buffer B: 20 mM Tris-HCl (pH 7.0), 200 mM KCl, 2 mM $MgCl_2$, and 1 mM DTT. [d] The rate of actin-activated phosphate release at 50 μM actin. [e] Apparent affinity, see Discussion and Scheme 4.

BTS thus has little effect on the rates of ATP binding and ATP hydrolysis by rabbit S1.

Rates of Phosphate Release (k_{+3d}, k_{+3a}). The rate of the conformational change that accompanies phosphate release from S1 in the absence of actin (k_{+3d}) was determined by single-turnover measurements. Substoichiometric concentrations of ATP were mixed with S1, and the decrease in the intrinsic tryptophan fluorescence was monitored as product phosphate was released. The time courses of fluorescence decreases follow single exponentials (Figure 3), with the rate constants 0.105 ± 0.004 s^{-1} in the absence of BTS, 0.012 ± 0.001 s^{-1} in the presence of 25 μM BTS, and <0.005 s^{-1} in the presence of 100 μM BTS. Therefore, BTS slows P_i release in the absence of actin >20-fold.

Fluorescently labeled P_iBP was used to measure the rate of phosphate release (k_{+3a}) in the presence of actin by sequential-mix, single-turnover, stopped-flow experiments (Figure 4). S1 (6 μM) was mixed with 3 μM ATP, aged for 1 s to allow for ATP binding and hydrolysis, and then mixed with phalloidin-stabilized actin. The final concentrations in the observation cuvette were 3 μM S1, 50 μM actin, and 1.5 μM ATP. Time courses of P_i release, measured by the fluorescence increase of the P_iBP in the absence of BTS, were best fit to the sum of two exponenital rates (k^{fast} = 53 ± 1.0 s^{-1}; k^{slow} = 9.6 ± 1.1 s^{-1}), and the amplitude of the fast phase was 85% of the total signal change (Figure 4*A*). It has been proposed that k^{fast} reports the rate of actin-activated P_i release (k_{+3a}^{app}), while k^{slow} reports the rate of ATP hydrolysis by actin-associated S1 (k_{+2a}; *18*). The steady-state ATPase rate is related to k_{2a}, k_{2d}, k_{3a}, k_6, and k_7 as previously described (*18*).

In the presence of 100 μM BTS, phosphate release transients at 50 μM actin were adequately fit by a single-exponential rate (k_{+3a}^{app} = 0.37 ± 0.01; Figure 4B). Thus, BTS slows actin-activated P_i release >100-fold. A two-exponential transient is not observed because BTS-inhibited P_i release is >100-fold slower than ATP hydrolysis (Table 1). In the presence of BTS, the rate of P_i release was within a factor of 2 of the steady-state ATPase rate determined for the same protein preparation.

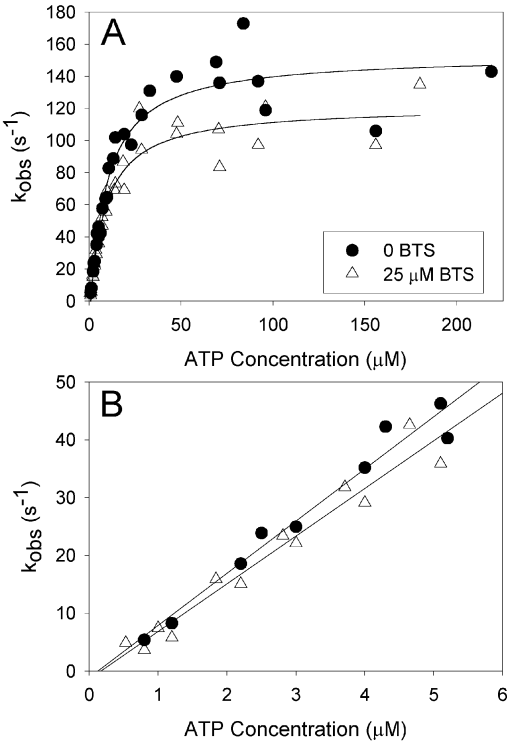

FIGURE 2: Increase of intrinsic tryptophan fluorescence of S1 upon binding of ATP. (A) Plot of the rate of increase of S1 tryptophan fluorescence upon mixing with ATP at concentrations of 1−220 μM in the absence of BTS (closed symbols) and in the presence of 25 μM BTS (open symbols). The final plateau gives the sum of the forward and reverse rates of ATP cleavage by S1. (B) The slope of a line fitted to the initial linear portion (ATP < 5 μM) is the second-order rate constant of ATP binding to S1. Final conditions were 1 μM S1, 10 mM imidazole (pH 7.0), 2 mM $MgCl_2$, 1 mM EGTA, 0.5 mM DTT, and 0 or 25 μM BTS. T = 25 °C.

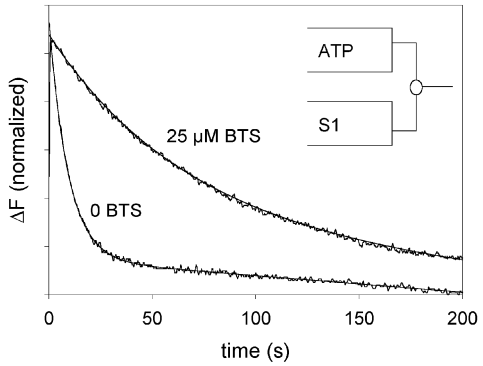

FIGURE 3: Single-turnover traces of ATP hydrolysis by rabbit S1 in the absence and in the presence of 25 μM BTS. Buffer conditions are the same as in Figure 2. Experiments were performed by mixing 2 μM S1 with 1 μM ATP. Rate constants were determined by fitting data to single-exponential curves.

Binding of S1 and S1·ADP to Pyrene-Actin. The fluorescence of pyrene-labeled actin was used to quantify the effect of BTS on the strong binding of S1 to actin (Figure 5). The fluorescence of pyrene-actin is not affected by 100 μM BTS or 1 mM ATP (bars B and C). Binding of subfragment 1 quenches pyrene-actin fluorescence to 35% of its initial value (D), as found in earlier studies (*21*), and the fluorescence recovers fully upon dissociation of S1 from actin by addition

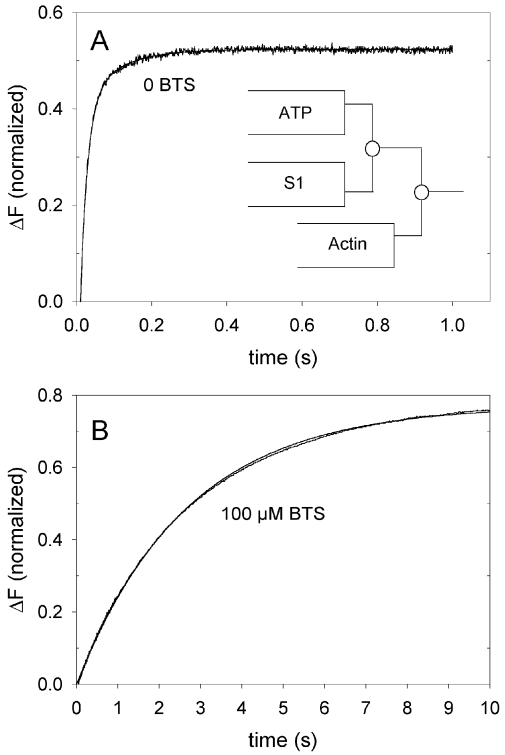

FIGURE 4: Phosphate release measured using fluorescently labeled P_iBP. Time course of P_i release from S1 in the presence of actin after mixing with ATP in a sequential mix, single-turnover experiment. Experiments were performed in the absence of BTS (A) and in the presence of 100 μM BTS (B). The smooth lines are exponential fits as described in the text. Final concentrations at $t = 0$ were 5 μM P_iBP, 1.5 μM ATP, 3.0 μM S1, 50 μM actin, 0.02 U/mL nucleoside phosphorylase, and 0.1 mM 7-methyguanosine. P_iBP was included with premix solutions of S1 and actin to prevent artifacts from phosphate released during the 1 s aging time. The buffer conditions are the same as in Figure 2.

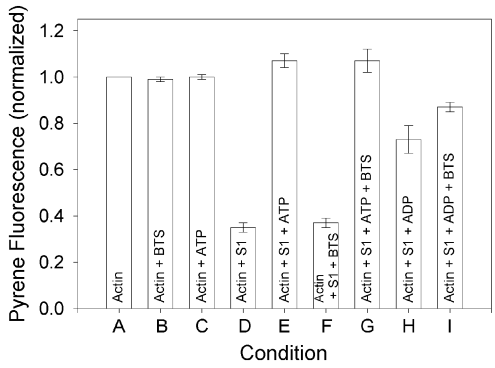

FIGURE 5: Pyrene-actin fluorescence measurements of acto-S1 under various conditions. Pyrene-actin fluorescence is normalized to 1. Final concentrations of individual components were 10 μM S1, 1 μM pyrene-actin, 1 mM ATP, 1 mM ADP, and 100 μM BTS. The buffer contained 20 mM Tris-HCl (pH 7.0), 200 mM KCl, 2 mM $MgCl_2$, and 1 mM DTT. In samples containing ADP, 20 U/mL hexokinase and 50 mM glucose were included to eliminate any contaminating ATP.

of 1 mM ATP (E). The same behavior is observed in the presence of 100 μM BTS. S1 decreases pyrene fluorescence to 37% of its initial value (F), suggesting that BTS does not affect the acto−S1 interaction and that actin is saturated with S1 under these conditions. Fluorescence was again fully recovered upon addition of 1 mM ATP (G). In the absence of BTS, 1 mM ADP partially dissociates S1 from actin,

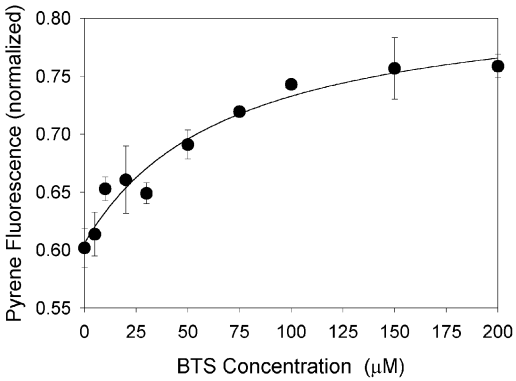

FIGURE 6: Dissociation of acto-S1·ADP by BTS. As [BTS] increases, pyrene fluorescence increases, indicating partial dissociation of S1·ADP from actin. Final concentrations were 10 μM S1, 1 μM pyrene-actin, 0−200 μM BTS, 20 mM Tris-HCl (pH 7.0), 200 mM KCl, 2 mM $MgCl_2$, and 1 mM DTT. The half-saturation value for S1·ADP dissociation from actin is 70 μM BTS.

increasing pyrene fluorescence to 73% of its initial value (H), consistent with ADP weakening the acto−S1 interaction. Upon addition of 100 μM BTS, the fluorescence further increases to 87% (I), indicating that BTS weakens acto−S1·ADP binding. This reduction of acto−S1 binding by BTS was observed in the presence of ADP but not in the absence of nucleotides under these conditions. The concentration dependence of the effect of BTS on S1·ADP binding to pyrene-actin followed a hyperbolic curve with a half-saturation value of 70 μM BTS (Figure 6). This concentration is >7-fold higher than the K_I for the suppression of the myosin ATPase activity.

Kinetics of Binding of S1 to Pyrene-Actin (K_5, k_{+5}, k_{-5}). The acto−S1 concentrations in the experiments of the previous section might be too high to permit detection of an effect of BTS on actomyosin affinity in the absence of nucleotide. Therefore, we determined the association (k_{-5}) and dissociation (k_{+5}) rate constants of S1 and actin in the presence and in the absence of BTS. The rate of association was measured by monitoring the decrease in pyrene-actin fluorescence upon mixing with S1. Both in the absence and in the presence of BTS, the observed fluorescent transients (k_{obs}) were best fit to the sum of two exponential rates. One of the two components is approximately 5-fold faster than the other, and they have approximately equal amplitudes. Figure 7A shows the rates of these two processes as a function of S1 concentration (closed symbols in the absence of BTS, open symbols in the presence of 100 μM BTS). The slopes of these plots provide the second-order rate constants of acto−S1 binding (k_{-5}). BTS has little effect on either the fast or slow component of S1 binding to actin (Table 1).

The dissociation rate constant (k_{+5}) was determined by mixing pyrene-acto-S1 with an excess of unlabeled actin. The fluorescent transients were best fit by single-exponential functions (Figure 7B). In the absence of BTS, dissociation proceeds at 0.29 s^{-1}, while in the presence of BTS, the rate is 0.31 s^{-1}. The calculated dissociation constants ($K_5 = k_{+5}/k_{-5}$) are 0.036 μM in the absence of BTS and 0.042 μM in the presence of BTS. These data confirm that BTS has little or no effect upon acto−S1 binding in the absence of nucleotide.

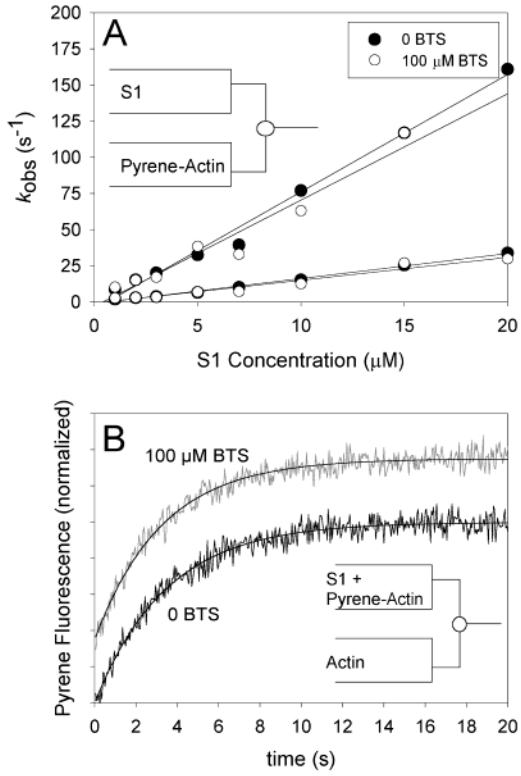

FIGURE 7: Pyrene-actin fluorescence upon binding and dissociation of S1. (A) Rate of pyrene-actin binding to 0−20 μM S1. Final conditions were 0.2 μM pyrene-actin, 0 (closed symbols) or 100 μM BTS (open symbols), 20 mM Tris-HCl (pH 7.0), 200 mM KCl, 2 mM $MgCl_2$, and 1 mM DTT at 25 °C. The data were best fit as double-exponential processes. (B) Fluorescence traces measuring the dissociation of pyrene-actin and S1 in the absence and in the the presence of 100 μM BTS (shifted upward for clarity). The rates of acto-S1 dissociation were measured by mixing acto-S1 (0.4 μM) with an excess of unlabeled actin (10 μM) in 20 mM Tris-HCl (pH 7.0), 200 mM KCl, 2 mM $MgCl_2$, and 1 mM DTT at 25 °C. Data were fit to single-exponential curves.

S1·ADP Binding to Pyrene-Actin (K_8). The apparent affinity of S1·ADP for pyrene-actin in the presence and in the absence of BTS was determined by steady-state titration (Figure 8). The decrease of the fluorescence from the equilibrium binding of S1 to pyrene-actin in the presence of 1 mM ADP was fitted by a rectangular hyperbolic function to obtain the dissociation constant of 7.0 ± 0.8 μM in the absence of BTS and 29 ± 5.6 μM in the presence of BTS.

Scheme 2

S1/ADP Association and Dissociation (K_{4d}). The interaction of ADP with rabbit S1 has been shown to be a two-step process (*22*) (Scheme 2). Initial ADP binding to S1 is followed by a conformational change to form the more fluorescent S1·ADP complex (M*·ADP in Scheme 2). If k_{-p} is rapid compared to k_{+q}, the rate at which this fluorescent complex is formed is described by

$$k_{obs} = \frac{k_{+q}[ADP]}{[ADP] + k_{-p}/k_{+p}} + k_{-q} \quad (1)$$

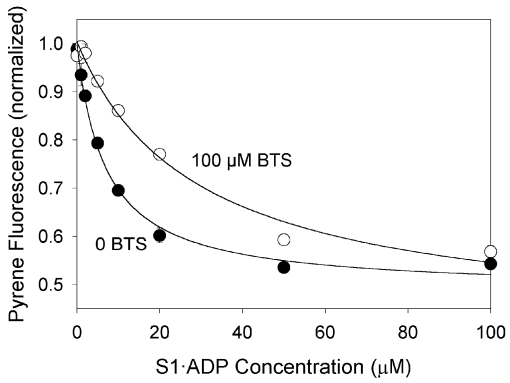

FIGURE 8: Steady-state fluorescence of pyrene-actin on binding 0−100 μM S1·ADP. Final concentrations were 1 μM pyrene-actin, 0 (closed symbols) or 100 μM BTS (open symbols), 20 mM Tris-HCl (pH 7.0), 200 mM KCl, 1 mM ADP, 2 mM $MgCl_2$, and 1 mM DTT.

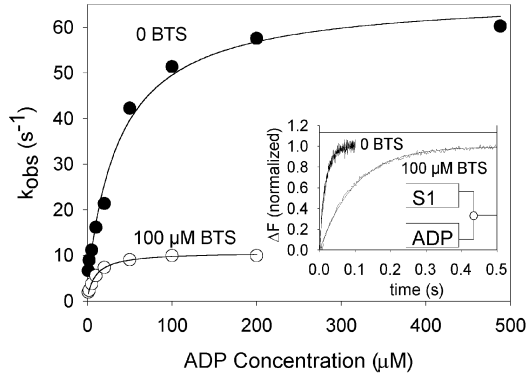

FIGURE 9: Rate of ADP binding to S1 as a function of ADP concentration via tryptophan fluorescence in the presence of 100 μM BTS (open symbols) and in the absence of BTS (closed symbols). The solid lines show eq 1 from the text fitted to the data. The inset shows examples of tryptophan fluorescence traces monitoring the binding of ADP by S1 in the absence of BTS and in the presence of 100 μM BTS at 200 μM ADP. Single-exponential curves are fitted to the time course of the fluorescence changes. Final conditions were 1.0 μM S1, 0−490 μM ADP, 20 mM Tris-HCl (pH 7.0), 200 mM KCl, 2 mM $MgCl_2$, and 1 mM DTT at 25 °C. The data are modeled as a two-step binding process (see text).

Figure 9 shows the experimentally determined rates of fluorescence enhancement observed upon mixing S1 with varying ADP concentrations both without and with BTS. Table 1 shows the rate constants obtained upon fitting eq 1 to the data. BTS affects every step of Scheme 2. It decreases the rate of the conformational change upon ADP binding (k_{+q}), but it increases the affinity of ADP for S1 in the initial rapid equilibrium step (k_{-p}/k_{+p}). As a result, the overall second-order rate constant of ADP binding [$K_p k_q = (k_{-p}/k_{+p})k_{+q}$] decreases less than 2-fold on addition of BTS.

To determine the magnitude of k_{-q} in the absence and in the presence of BTS, we mixed S1·ADP with excess ATP. Under these conditions, ADP is released from the active site, and then ATP binds and is cleaved to form ADP·P_i. The S1·ADP·P_i complex exhibits higher fluorescence than S1·ADP alone. The rate-limiting step of this process is k_{-q} (*22*). In the absence and in the presence of BTS, the increase in fluorescence followed single-exponential time courses with rate constants of 3.9 ± 0.03 and 0.8 ± 0.02 s^{-1}, respectively (Figure 10). Combining these values, the overall dissociation constant of ADP binding ($K_{4d} = k_{-p}k_{-q}/k_{+p}k_{+q}$) is reduced

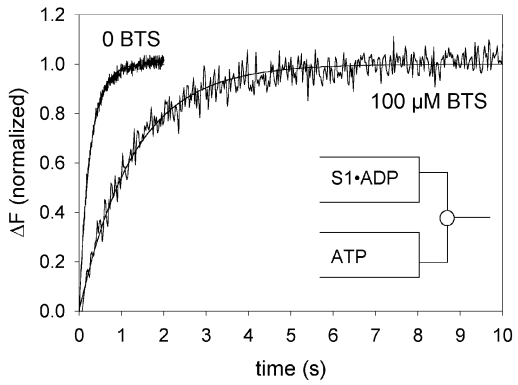

FIGURE 10: Tryptophan fluorescence traces monitoring the release of ADP by S1 in the absence of BTS and in the presence of 100 μM BTS. In the reaction, 10 μM ADP was chased off the enzyme by 2 mM ATP. Final conditions were 1.0 μM S1, 20 mM Tris-HCl (pH 7.0), 200 mM KCl, 2 mM $MgCl_2$, and 1 mM DTT at 25 °C. The traces were fit by single-exponential kinetics.

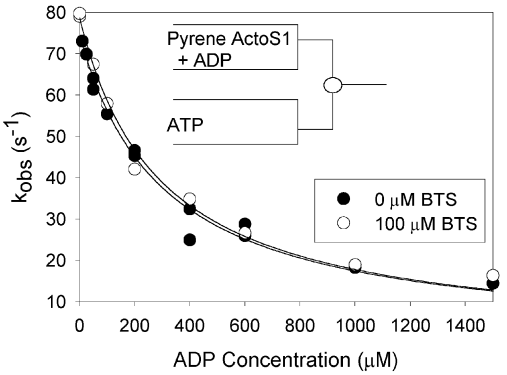

FIGURE 11: Affinity of ADP for acto-S1 in the absence of BTS (closed symbols) and in the presence of 100 μM BTS (open symbols). The rate of pyrene-acto−S1 dissociation by 40 μM ATP was measured as a function of ADP concentration. Final concentrations were 0.6 μM S1 and 0.5 μM pyrene-actin in 20 mM Tris-HCl (pH 7.0), 200 mM KCl, 2 mM $MgCl_2$, and 1 mM DTT.

approximately 3-fold in the presence of BTS. k_{-q} is also given by the ordinate intercept of the curves in Figure 9. The values of k_{-q} given by this intercept are consistent with those obtained from the experiments of the type shown in Figure 10.

BTS affects the amplitudes of the tryptophan fluorescence signals in both the ADP association and dissociation experiments described above. The increase in fluorescence upon ADP binding is enhanced approximately 3-fold in the presence of BTS (not shown). Conversely, the difference in tryptophan fluorescence of the ADP and ADP·P_i bound states, used to measure the rate of ADP release, is about 3-fold smaller in the presence of BTS. We found that BTS increases the intrinsic fluorescence of M·ADP by 10−20%. The changes in amplitude of the transient fluorescence signals on binding or dissociation of nucleotides are consistent with the effect of BTS on M·ADP fluorescence.

Scheme 3

ADP Binding to Pyrene-Acto-S1 (K_{4a}). We determined the dissociation constant for ADP binding to acto-S1 by measuring the extent of inhibition of ATP-induced acto−S1 dissociation as a function of ADP concentration (Scheme 3; *23*). At low ATP concentrations, such that ATP association is slow compared to ADP association, the ADP-binding step is approximately at equilibrium, and the rate of ATP-induced acto−S1 dissociation is described by

$$k_{obs} = \frac{k_{1a}[ATP]}{1 + [ADP]/K_{4a}} \quad (2)$$

where k_{1a} is the rate of acto−S1 dissociation in the absence of ADP. In the absence of ADP, the rate of acto−S1 dissociation induced by 40 μM ATP is 76.7 ± 0.6 s^{-1} in the absence of BTS and 73 ± 3.7 s^{-1} in the presence of BTS. The second-order rate constant for ATP binding (k_{1a}) was thus calculated to be (1.9 ± 0.02) × 10^6 M^{-1} s^{-1} in the absence of BTS and (1.8 ± 0.09) × 10^6 M^{-1} s^{-1} in the presence of BTS. As in the case of ATP binding to S1 alone, BTS does not greatly affect the binding of ATP to acto-S1.

As the ADP concentration is increased, k_{obs} declines (Figure 11) both with (open symbols) and without BTS (closed symbols). Fits of eq 2 to the data yielded an association constant of K_{4a} = (3.3 ± 0.3) × 10^3 M^{-1} in the absence of BTS and K_{4a} = (3.4 ± 0.5) × 10^3 M^{-1} in the presence of BTS. Thus, BTS does not affect the affinity of ADP for acto-S1, even though it strengthens the binding of ADP to S1 alone.

DISCUSSION

BTS has previously been shown to inhibit contraction in fast skeletal muscle fibers (*1*). At saturating concentrations, BTS decreases active isometric tension and stiffness in rabbit psoas fibers while only slightly affecting unloaded shortening velocity. Mechanical transients initiated by quick length changes were reduced in amplitude by BTS, but the kinetics of force recovery after the length changes were not markedly altered (*1*, *24*). The simplest explanation of these results is that BTS decreases the number of actomyosin attachments during active contraction without otherwise altering the transition rates between mechanical steps of the cross-bridge cycle.

We found that BTS reduces the S1 MgATPase rate, the acto-S1 MgATPase rate, the affinity of ADP for S1, and the affinity of the S1·ADP complex for actin. ATP binding and hydrolysis by S1 were not affected much by BTS, but P_i release from S1·ADP·P_i and acto-S1·ADP·P_i was suppressed sufficiently to account for the reduction of the overall ATPase rates in the absence and in the presence of actin. The decreased K_{ATPase} also suggests a weakened affinity of S1·ADP·P_i for actin. This reduced affinity contributes to the ATPase suppression at intermediate actin concentrations. ATP and ADP binding to acto-S1 and the affinity of nucleotide-free S1 for actin were not altered by BTS.

The equilibrium constants K_{4d}, K_8, and K_{4a} are well defined by the experimental data. The backward component of K_5, conversely, is comprised of separate fast and slow processes of approximately equal amplitude. The fast process is close to prior literature values for S1 binding to actin (*25*). The law of detailed balance can be used as a check of consistency of experimental rate constants and the kinetic model used

Scheme 4

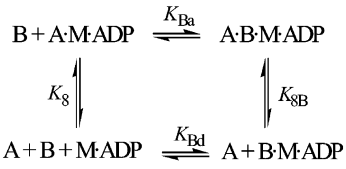

for analysis. In any closed kinetic system, the product of the equilibrium constants of that system equals one: $K_{4d}K_8/K_{4a}K_5 = 1$. Using the experimental values for K_{4d}, K_8, and K_{4a} and the fast phase of k_{-5} for calculation of K_5 yields values for the above ratio of 1.44 and 1.90 without and with BTS, respectively. Using the slow component of k_{-5}, these values are 0.31 and 0.42, respectively.

The concentration of BTS which half-saturates the dissociation of M·ADP from actin (70 μM, Figure 6) is more than 7-fold greater than the K_I of BTS for ATP hydrolysis either in the absence or in the presence of actin (8 and 3 μM, respectively). This difference can be explained if the affinity of BTS is different for various states of the ATPase cycle. Dissociation of AM·ADP by BTS can be considered in more detail as shown in Scheme 4, where B indicates BTS, B·M·ADP and A·B·M·ADP are the respective complexes with BTS, and the four equilibrium constants are dissociation constants. The half-saturation value for dissociation of M·ADP from actin, and the apparent AM·ADP affinity in the absence of BTS and in the presence of 100 μM BTS (K_8 in Table 1), provide sufficient information to estimate all of the dissociation constants in Scheme 4: $K_8 = 7$ μM, $K_{8B} = 314$ μM, $K_{Bd} = 27$ μM, and $K_{Ba} = 1200$ μM, although the uncertainties on K_{8B} and K_{Ba} are large. This analysis indicates that the complex of BTS and M·ADP binds weakly, if at all, to actin and that BTS either does not bind to AM·ADP or binds much more weakly than to M·ADP. BTS may not bind to AM, either. It seems to bind tightly to M·ADP·P_i and AM·ADP·P_i according to the potent inhibition of the ATPase activity. Thus, the binding of BTS to myosin depends on the other ligands bound and/or the conformation of the myosin molecule.

Taken together, the data suggest that BTS affects the kinetics of ATP hydrolysis in two distinct ways. First, BTS decreases the rate of phosphate release from myosin both in the presence and in the absence of actin. Second, BTS weakens the apparent acto-S1 affinity in the S1·ADP·P_i and S1·ADP states (but not apo-S1). Reduction of P_i release from the actomyosin products complex and decreased affinity of myosin for actin provide explanations for the suppression of active tension in fibers. That ADP release from acto-S1·ADP was not affected by BTS is compatible with the nearly unaltered maximum shortening velocity in psoas fibers (*1*).

To quantitatively relate the observations on isolated actomyosin to the effects of BTS on muscle fiber contraction, several differences between the two systems need to be taken into account. The isolation procedure and proteolytic cleavage to produce S1 might alter some steps of the enzymatic activity. Mechanical stress and strain characteristic of the fiber contraction are not present in the biochemical experiments. The actin concentrations used with the isolated proteins (up to 200 μM) are much lower than the bulk actin concentration within the overlap zone of the intact sarcomere ($\sim$1 mM), and the geometrical arrangement of the filaments may raise the "effective actin concentration" even higher (*26*). Thus, prediction of the expected extent of force suppression by BTS on the basis of the rate constants observed with acto-S1 is not straightforward. In the simplest case, in which the force generated by each attached cross-bridge is the same in the presence and in the absence of BTS and all of the myosin heads are available for cross-bridge cycling, the force and stiffness would be proportional to the number of attachments. Then the proportion of cross-bridges attached at any instant is given by $P = f/(f + g)$, where f is the transition rate into the strongly bound, force-generating state and g is the transition rate out of this state (*27*). If we initially assume that the rate of P_i release from AM·ADP·P_i (k_{3a}, Scheme 1) controls f, then the reduction of the actomyosin ATPase from 23.3 to 2.5 s^{-1} (at V_{max}) in the presence of BTS can provide an initial estimate of the expected force reduction. Taking g as a constant value at 25 s^{-1}, then $P = 0.48$ and 0.09 in the absence and in the presence of BTS, respectively, giving an expected tension in the presence of BTS that is 19% (0.09/0.48) of the control tension. If g has a constant value at 130 s^{-1}, then $P = 0.15$ and 0.019, giving an expected tension in the presence of BTS of 13% of the control. However, Cheung et al. (*1*) reported that BTS suppressed tension to 3% of its control level, a much greater suppression than these values.

The reduced affinity of the strongly bound AM·ADP intermediate for actin in the presence of BTS might contribute further to tension suppression. The concentration of actin present in the muscle fiber, however, is well above the apparent dissociation constants for M·ADP binding to actin in the absence (7.0 μM) and in the presence (29 μM) of BTS, suggesting that virtually all M·ADP intermediates would be bound to actin in both cases. Mechanical strain on the force-generating intermediates could weaken the affinity, allowing this factor to play a role.

Alternatively, the cross-bridge detachment rate (g) might depend on BTS. For instance, if g increases 4-fold, from 130 to 520 s^{-1}, on addition of BTS, then $P = 0.15$ and 0.0048, and tension in the presence of BTS would be 3% of the control, as reported. A disadvantage of this idea is that the shortening velocity of the fiber might be expected to increase in BTS, which was not observed. The number of myosin heads available for cycling or the rate of entry into the force-generating state might be altered by BTS more than the 10-fold reduction of the ATPase rate. Thus, the kinetics observed with S1 only partly explain the effectiveness of tension suppression by BTS, and further changes, possibly mediated through mechanical stress or strain, may alter the cross-bridge cycle in fibers. BTS detached rigor cross-bridges in muscle fibers but did not affect nucleotide-free S1 affinity for actin, again suggesting strain dependence of the effects of BTS.

The specific steps of ATP hydrolysis modulated by BTS may provide insight into the structural interaction of BTS with S1 and acto-S1. The actin-binding 50-kDa domain of myosin is split by a large cleft that extends from the presumed actin-binding site to the base of the nucleotide-binding site (*28*). This cleft has been postulated to close on actin binding (*29*). Phosphate release has been postulated to occur via a "backdoor" or secondary exit from the protein's active site into the base of the same 50-kDa cleft (*30*). Thus, if BTS binds within this cleft, it might block release of P_i

and hinder closing of the cleft and, consequently, actin binding.

Motions of protein segments around the 50-kDA cleft have been proposed to provide coupling between the nucleotide-bound state of S1 and actin affinity (*28*, *29*). From cryo-electron micrographic reconstructions of decorated actin, Volkmann et al. (*31*) detected a partial opening upon binding of ADP to actomyosin. BTS binding thus might be blocked in the nucleotide-free rigor actomyosin complex relative to the AM·ADP state. These conjectures are consistent with our results that BTS does not affect rigor acto−S1 binding in solution but does affect binding of actin and S1·ADP.

BTS decreases force in fast skeletal muscle fibers, but the tension recovery following quick length changes is not markedly altered (*1*). The quick tension recovery is thought to signal the elementary step of force production (*32*), which has also been linked to release of P_i from AM·ADP·P_i (*33*, *34*). Here we present evidence that release of P_i from AM·ADP·P_i is suppressed by BTS. Thus, the relatively normal rate of the quick tension recovery in the presence of BTS provides evidence that force generation and P_i release are not simultaneous. A sequential mechanism of force generation followed by quick release of P_i from force-generating AM·ADP·P_i cross-bridges (*35*, *36*) can account for this decoupling by BTS of force generation and P_i release.

In conclusion, the ability of BTS to decrease tension in actively contracting fast skeletal muscle fibers can be attributed to at least two actions. First, it decreases the rate of phosphate release from both S1 and acto-S1 and presumably does the same in the fiber. Second, it decreases the affinity of S1·ADP·P_i and S1·ADP for actin. Both of these effects would decrease the number of cross-bridges bound to the thin filament during active contraction, thus decreasing the sliding force exerted between the filaments. It is possible that BTS exerts these two effects by binding within the open conformation of the 50-kDa cleft while S1 is dissociated from actin.

ACKNOWLEDGMENT

We thank Tianming Lin for technical assistance, and Drs. Jody Dantzig, Joseph Forkey, Henry Shuman, and Margot Quinlan for useful discussions. We also thank Drs. Tim Mitchison and Aaron Straight for their gift of BTS, and Dr. Steven Rosenfeld for providing P_iBP.

REFERENCES

1. Cheung, A., Dantzig, J. A., Hollingworth, S., Baylor, S. M., Goldman, Y. E., Mitchison, T. J., and Straight, A. F. (2002) *Nat. Cell Biol. 4*, 83−88.
2. Higuchi, H., and Takemori, S. (1989) *J. Biochem. 105*, 638−643.
3. Siegman, M. J., Mooers, S. U., Warren, T. B., Warshaw, D. M., Ikebe, M., and Butler, T. M. (1994) *J. Muscle Res. Cell Motil. 15*, 457−472.
4. Ostap, E. M. (2002) *J. Muscle Res. Cell Motil. 23*, 305−308.
5. Sellin, L. C., and McArdle, J. J. (1994) *Pharmacol. Toxicol. 74*, 305−313.
6. Trentham, D. R., Eccleston, J. F., and Bagshaw, C. R. (1976) *Q. Rev. Biophys. 9*, 217−281.
7. Taylor, E. W. (1979) *CRC Crit. Rev. Biochem. 6*, 103−164.
8. Eisenberg, E., and Greene, L. E. (1980) *Annu. Rev. Physiol. 42*, 293−309.
9. Hibberd, M. G., and Trentham, D. R. (1986) *Annu. Rev. Biophys. Biophys. Chem. 15*, 119−161.
10. Goldman, Y. E. (1987) *Annu. Rev. Physiol. 49*, 637−654.
11. Geeves, M. A., and Holmes, K. C. (1999) *Annu. Rev. Biochem. 68*, 687−728.
12. Shaw, M. A., Ostap, E. M., and Goldman, Y. E. (2002) *Biophys. J. 82*, 377a.
13. Wagner, P. D., and Yount, R. G. (1975) *Biochemistry 14*, 1900−1907.
14. Okamoto, Y., and Sekine, T. (1985) *J. Biochem. 98*, 1143−1145.
15. Grammer, J. C., Cremo, C. R., and Yount, R. G. (1988) *Biochemistry 27*, 8408−8415.
16. Pardee, J. D., and Spudich, J. A. (1982) *Methods Enzymol. 85*, 164−181.
17. Pollard, T. D. (1984) *J. Cell Biol. 99*, 769−777.
18. White, H. D., Belknap, B., and Webb, M. R. (1997) *Biochemistry 36*, 11828−11836.
19. Brune, M., Hunter, J. L., Corrie, J. E. T., and Webb, M. R. (1994) *Biochemistry 33*, 8262−8271.
20. Johnson, K. A., and Taylor, E. W. (1978) *Biochemistry 17*, 3432−3442.
21. Criddle, A. H., Geeves, M. A., and Jeffries, T. (1985) *Biochem. J. 232*, 343−349.
22. Bagshaw, C. R., Eccleston, J. F., Eckstein, F., Goody, R. S., Gutfreund, H., and Trentham, D. R. (1974) *Biochem. J. 141*, 351−364.
23. Siemankowski, R. F., and White, H. D. (1984) *J. Biol. Chem. 259*, 5045−5053.
24. Linari, M., Piazzesi, G., and Lombardi, V. (2002) *Biophys. J. 82*, 377a.
25. Taylor, E. W. (1991) *J. Biol. Chem. 266*, 294−302.
26. Pate, E., and Cooke, R. (1988) *Biophys. J. 53*, 561−573.
27. Huxley, A. F. (1957) *Prog. Biophys. Biophys. Chem. 7*, 255−318.
28. Rayment, I., Rypniewski, W. R., Schmidt-Bäse, K., Smith, R., Tomchick, D. R., Benning, M. M., Winkelmann, D. A., Wesenberg, G., and Holden, H. M. (1993) *Science 261*, 50−58.
29. Rayment, I., Holden, H. M., Whittaker, M., Yohn, C. B., Lorenz, M., Holmes, K. C., and Milligan, R. A. (1993) *Science 261*, 58−65.
30. Yount, R. G., Lawson, D., and Rayment, I. (1995) *Biophys. J. 68*, 44s−49s.
31. Volkmann, N., Hanein, D., Ouyang, G., Trybus, K. M., DeRosier, D. J., and Lowey, S. (2000) *Nat. Struct. Biol. 7*, 1147−1155.
32. Huxley, A. F., and Simmons, R. M. (1971) *Nature 233*, 533−538.
33. Hibberd, M. G., Dantzig, J. A., Trentham, D. R., and Goldman, Y. E. (1985) *Science 228*, 1317−1319.
34. Cooke, R., and Pate, E. (1985) *Biophys. J. 48*, 789−798.
35. Dantzig, J. A., Goldman, Y. E., Millar, N. C., Lacktis, J., and Homsher, E. (1992) *J. Physiol. 451*, 247−278.
36. Kawai, M., and Halvorson, H. R. (1991) *Biophys. J. 59*, 329−342.

BI026964F